A Fast Scheme for Fault Detection in DC Microgrid Based on Voltage Prediction

Anju Meghwani, Saikat Chakrabarti, S. C. Srivastava
Department of Electrical Engineering
Indian Institue of Technology Kanpur
Kanpur, UP, India, 208016
Email: anjum@iitk.ac.in, saikatc@iitk.ac.in, scs@iitk.ac.in

***Abstract*—Protection schemes for AC transmission systems are well understood and matured. On the other hand, developing proper protection scheme for DC system is still a research challenge. A distributed fault detection and localization scheme, based on local measurements, is proposed in this paper. It is based on the fact that a fault generally leads to a significant drop in the voltage along with its high rate of change. The voltage at the fault point is predicted using a quadratic time varying function. In case of fault, the difference in the predicted and the true values exceeds certain threshold. A systematic procedure for setting the necessary threshold value is also suggested. The protection system has been modelled and tested for different fault types, their locations. and with the noisy measurement. The proposed scheme is validated on a ring type DC microgrid system using Real Time Digital Simulator (RTDS).**

Index Terms - DC Microgrid, DC system protection, voltage measurement, voltage prediction.

I. Introduction

A low or medium voltage electrical network, consisting of distributed resources, especially renewable sources of energy, storage devices, and loads, is known as a Microgrid [1]. The electrical network can be AC, DC, or mixed of the two, and may or may not be connected to the main grid. The DC distribution system has advantage of high efficiency [2], easy paralleling of sources on DC bus [3], and more power transfer capacity [4].

One of the main challenges in adopting the DC distribution system is the lack of effective solution to the fault protection. DC microgrid may consist of Voltage Source Converters (VSCs) in the network, which demand fast protection and isolation of the faulted section from the network. Because of the presence of large DC capacitors and low impedance offered by the DC cable, a fault in the DC system may result into high transient currents and voltages.

A protection scheme based on signal handshake method for Multi Terminal DC system is reported in [5]. In this scheme, as the fault is detected, all the VSCs are disconnected from the AC side, and the capacitors on the DC side support the load for short duration. As the system de-energises, the load is dropped during the fault, which is not a desired situation. Reference [6] studied the application of different system parameters, such as over current, under voltage, di/dt, dv/dt during the faults. The results illustrate that the peak magnitude and the time to reach the peak of the fault current is the same for over and under damped fault conditions. This implies that the response is less dependent on the fault type and, thus, makes the fault discrimination difficult.

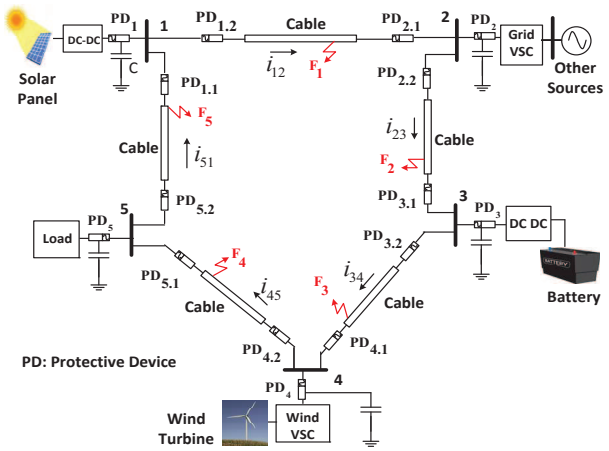

Fig. 1. A ring type DC microgrid architecture

Reference [7] had investigated a range of protection solutions and reported that the differential current scheme is suitable for the DC system. Differential protection has highest selectivity, and operates only in case of internal fault. Its operation would not be affected by size and rating of the system components. But it requires a reliable communication channel for instantaneous data transfer between the terminals of the protected element. Because of possible communication failure, differential protection will require a separate backup protection scheme. This increases the total cost and size of the protection system, and limits its application in the microgrids.

The concept of smart grid and microgrid requires sensors and communication networks to be provided in order to monitor the system condition and avoid outages. The communication may not be critical for monitoring functions, but its failure in protection system may result into system shutdown. This paper proposes a protection scheme based on local measurements and system parameter characteristics, which does not require any communication network. A mathematical model is developed to predict the voltage at the relay point. A protection system design framework is developed, which provides fault discrimination at faster speed. The proposed

scheme is tested on a typical DC microgrid architecture shown in Fig. 1.

II. System Analysis During Fault

Considering the high rate of rise of current under fault in a highly capacitive DC grid, it is important to detect the fault as soon as possible and trip the breakers. Although over current is a good indicator of a fault, waiting for the current to exceed a threshold introduces delay in trip signal, which may result in high rating of circuit breakers.

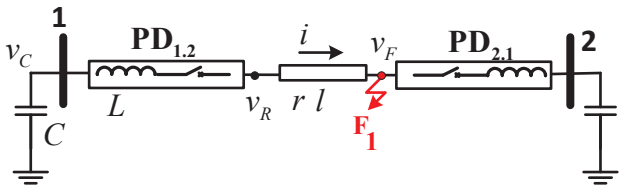

Fig. 2. Faulted network section

Another possibility is to utilize the rate of change of current to detect the fault [8]. Each DC breaker has an inductor in series with it to limit the rate of rise of current [9], [10]. The rate of change of current is given by,

$$\frac{di}{dt} = \frac{v_C(t) - v_R(t)}{L} \tag{1}$$

where L is the inductance of the di/dt limiting inductor and v_C and v_R are the voltages on the bus and line side of the Protective Device (PD) [11], [12], as shown in Fig. 2. The voltage on the bus side of a PD, v_C, remains relatively constant for few microseconds such as samples 1335 to 1355 shown in Fig. 3. As a result, the rate of change of current seen by the breaker is proportional to the voltage change on the line side of the PD and can be replaced by the line side voltage measurement v_R.

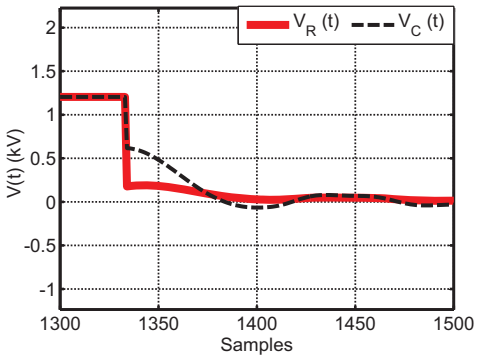

Fig. 3. Plots of v_R and v_C fault F_1

The solution proposed in this paper is to utilize voltage, measured at line side of the PD, to detect and isolate the fault. The method is based on the difference in the measured and predicted voltage values. The voltage at the relay point v_R has been predicted using Vandermonde matrix [13]. Because of the presence of high dv/dt, the change will be large. Other option is to utilize the rate of change of voltage itself to discriminate the faults in the network. The change in the voltage Δv is calculated using predicted voltage and the actual voltage i.e.,

$$\Delta v_R(t) = v_R(t) - v_R(t-1) \tag{2}$$

$$\Delta v_{RP}(t) = v_{RP}(t) - v_R(t) \tag{3}$$

where, $\{v_R(t); v_{RP}(t)\}$ are the measured and predicted voltage at time t; $\{\Delta v_R; \Delta v_{RP}\}$ are the change in voltages at time t. Time t and $t-1$ represent the present and one sampled previous data, respectively. From Fig. 4, it is found that Δv_R, which depends on the measured parameter, dies out quickly. It may cause difficulty in taking the decision based on the single point measurement. Also, the maximum value of Δv_{RP} is large as compared to Δv_R. Due to this, it is easy to set the pick up threshold for PDs connected with different cable lengths.

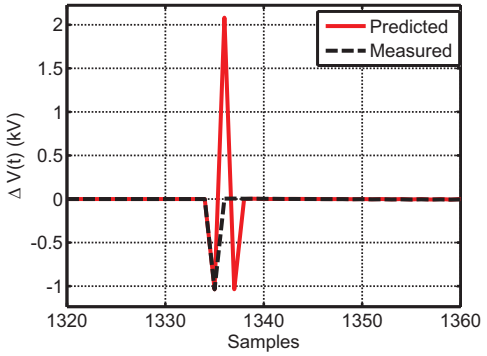

Fig. 4. Plots of $\Delta v_R(t)$ and $\Delta v_{RP}(t)$ during fault F_1

III. Quadratic Model

In this section, a quadratic model of the voltage at line side of the breaker is developed. In this model, the next data point is predicted using the previous data points [13]. Determining the inverse of a Vandermonde matrix for a 2^{nd} order polynomial yields a set of coefficients, which can interpolate or predict the next data point. This prediction polynomial is quadratic in nature and can be used to predict future voltage from the historical trend. To develop the model, consider a fault F_1 as shown in Fig. 2,

$$v_R = v_F + l\frac{di}{dt} + ir \tag{4}$$

where, $\{r; l\}$ are the cable inductance and resistance; $\{v_R; v_F\}$ are the voltages at the PD and fault point, and i is the line current. On integrating (4) from time $t = 0$ (when fault occurs) to t, the change in the line current Δi can be written as,

$$\Delta i = \frac{(v_R - v_F)t - irt}{L} \tag{5}$$

On multiplying both sides by the line current, one gets,

$$i^2 rt + iL\Delta i + (P_F - P_R)t = 0 \tag{6}$$

where, $\{P_F; P_R\}$ are the power at fault point and power measured at the line side of the PD. The difference in the

power is constant and varies with time t during fault. The line current $i(t)$ is a quadratic polynomial, which can be written as,

$$i(t) = \frac{-L\Delta i \pm \sqrt{(L\Delta i)^2 - 4(P_F - P_R)rt^2}}{2rt} \quad (7)$$

Since line current $i(t)$ is a quadratic function of time, the voltage at relay point is also a quadratic function of time t. Because $v_R(t)$ is quadratic, three previous data points, spread equally in time, would be required.

$$\beta_t v_R(t) + \beta_{t-1} v_R(t-1) + \beta_{t-2} v_R(t-2) + \beta_{t-3} v_R(t-3) = 0; \quad (8)$$

For $t = 3$, the coefficients of the quadratic prediction polynomial are $\beta = \{-1; 3; -3; 1\}$ and, therefore, $v_R(t)$ can be written as,

$$v_{RP}(t) = 3v_R(t-1) - 3v_R(t-2) + v_R(t-3) \quad (9)$$

The polynomial function (9) is a quadratic function and depends upon the previous two sampled data. This is applied in different scenario of DC microgrid to check its applicability. The aim is to demonstrate the accuracy of the method to predict the voltage during normal operation and different operating modes, such as transition from grid to islanded mode or vice-versa or during the load variations.

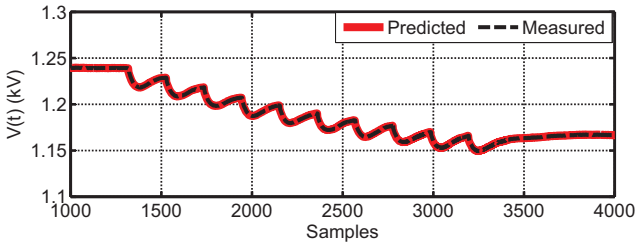

Fig. 5. Plots of v_{RP} and v_R when load varies with time

A. Load Variation

Fig. 5 shows the voltage trajectory ($v_R(t)$) on line side of the breaker. In this study, the load was increased with time and plotted against the number of samples. It can be seen that the quadratic function for v_{RP} tracks the actual voltage v_R with high accuracy. The prediction is accurate and consistent with the change in the operating point of the system.

B. Mode Transition

The DC microgrid can operate in either grid connected or in islanded mode. To simulate the microgrid in different modes, the breaker connected between the grid VSC and the bus 2 is operated. In both the cases, there is a transient in the system and causes disturbance. The predicted voltage v_{RP}, based on quadratic polynomial (9), is able to track the voltage trajectory $v_R(t)$, as shown in Fig. 6. The difference between the actual and the predicted voltage is much less than the threshold for few sampling period and then it settles to a the steady state value.

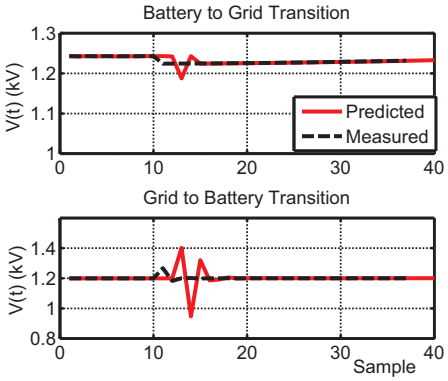

Fig. 6. Plots of v_{RP} and v_R during mode transitions

IV. Fault Analysis

Different cases are simulated to test the robustness of the polynomial function v_{RP}, such as load variation and operating mode transitions. These transitions are normal and do not include any sudden change in the voltage or the current. On the other hand, in case of a fault, there is a sudden change in the voltage with high dv/dt. Mathematically, it is difficult to track such transients. To study the quadratic polynomial behaviour in fault cases, faults are simulated at various locations, F_1 to F_5, as shown in Fig. 7.

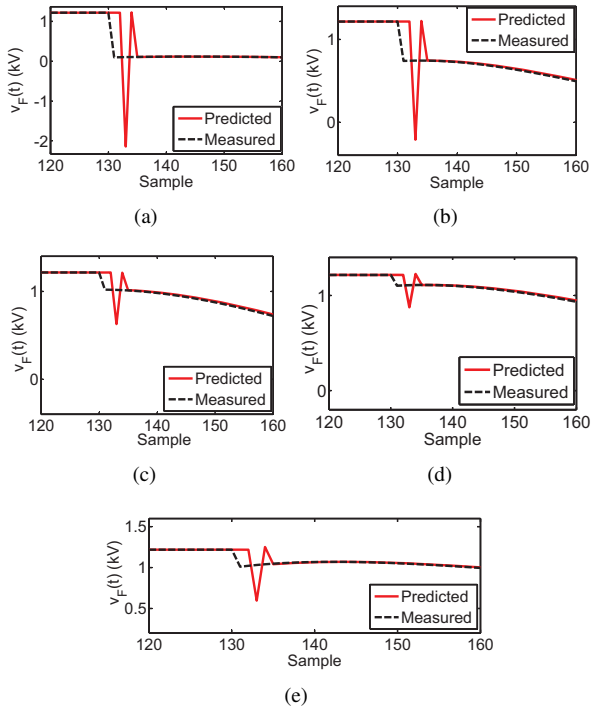

Fig. 7. Voltages v_{RP} and v_R measured at $PD_{1.2}$ for fault at locations (a)F_1, (b)F_2, (c)F_3, (d)F_4, and (e)F_5

The voltage $v_R(t)$ at $PD_{1.2}$ is measured for all the fault cases. The quadratic polynomial for the voltage prediction (9) is applied in the fault scenario, as shown in Fig.7. It can be seen that there is a significant difference between the predicted

voltage and the actual measurement in case of the fault. The small cable impedance and large filter capacitance cause high rate of rise of current. As a result, there is large rate of drop in the voltage. The quadratic polynomial tries to fit with the actual data and takes few samples to track the actual measurement.

Since the voltage prediction is based on the previous sampled data, as the fault occurs, there will be large difference between the measured and the predicted data because of the quadratic function characteristics. The difference between the predicted and the actual voltage depends upon the network and the fault parameters, such as fault resistance, and fault location. As the fault distance increases, the difference in the magnitudes reduces, as observed in Figs. 7(a)-(e). This difference in the voltage is considered as fault indices to identify the faults and their severity. For example, for the fault F_1, the difference between the two voltages is more than 3 p.u., as shown in Fig. 7(a), while for the fault F_5, it is 0.6 kV only as given in Fig. 7(e). This implies that the fault F_1 is in the vicinity of the voltage sensing point at cable 1-2.

TABLE I
MAXIMUM CALCULATED ΔV_{RP} AND ΔV_R AT $PD_{1.2}$ FOR DIFFERENT FAULT LOCATIONS

Faults	Distance from PD (m)	Δv_{RP} (kV)	Δv_R (kV)
	0	3.7	1.2
F_1	250	2	0.6
	500	3.6	1.2
F_2	-	1.2	0.5
F_3	-	0.5	0.2
F_4	-	0.3	0.1
F_5	-	0.6	0.2

V. PROTECTION DESIGN

The most important part of the complete protection system design lies in the coordination of relays. The proposed scheme for selection of threshold value and protection coordination is discussed in the following sections.

A. ΔV Threshold Setting

In this paper, PDs connected at both the ends of the cables define the zone of protection as shown in Fig. 1. PD consists of DC circuit breaker, relay and voltage measurement circuit. The voltage at the relay location is sampled, and is also predicted using the previous three samples (9). As the fault occurs, the voltage v_F becomes zero. At $t = 0^+$, voltage v_R can be written as,

$$v_R(t) = l\frac{di}{dt} + ir \tag{10}$$

At $t = 0^+$, $v_R(t) = 0$, since the cable resistance and inductance are very small. Because of the presence of di/dt limiting inductor, the fault current will not rise and will not contribute to the $v_R(t)$. The previous sampled data $v_R(t-1)$ to $v_R(t-3)$ are 1 pu as the grid was normally operating. As a result, v_{RP} becomes 1 pu, which results in $\Delta v_{RP} = 1pu$. Hence, the threshold setting for Δv_{RP} for the PDs will be 1 pu. The calculated threshold values are independent of the operating mode of the DC microgrid.

B. Coordination of PDs

In this case study, the fault points to be differentiated are F_1 to F_5. Since the ring type microgrid architecture is considered, any fault on the grid can be fed from either one or two sources. For example, fault F_1 to F_3 will be fed by sources on both the sides, while faults F_4 and F_5 from a single source. First task would be to pick up the parameter that best differentiates the faults and the second task is to select the appropriate breaker to open and isolate the fault.

From Fig. 7(a)-(e), it is clear that the difference between the estimated and measured voltage is maximum for the faults in the vicinity of $PD_{1.2}$. For the faults away from PD, the difference is quite less, as shown in Fig. 7. Moreover, the voltage difference Δv_{RP} remains constant for the faults out of reach of PD because it does not depend on the absolute value of the voltage or the current.

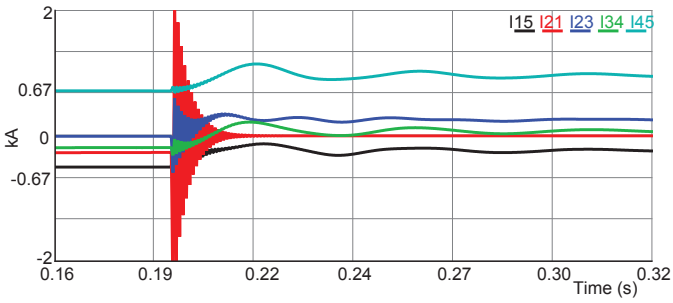

Fig. 8. Line currents after fault F_1 is cleared by $PD_{1.2}$ and $PD_{2.1}$

VI. VALIDATION ON RTDS

To demonstrate the proposed protection scheme, fault F_1 in the ring type microgrid, as shown in Fig. 1 was first simulated on the RTDS. A high transient current causes voltage collapse within 5 ms of the fault occurrence. This implies that the protection required for the DC system should be much faster as compared to the AC system [3]. The PDs connected on the cable continuously sample and monitor the voltages. After the fault F_1, Δv_{RP} is calculated using the previous and the present sampled voltages, and compared with the threshold calculated in the above section, to generate the trip signal. $PD_{1.2}$ and $PD_{2.1}$ operate and disconnect the faulted line, thereby restoring the system, as shown in Fig. 8.

The proposed scheme is tested and validated for the faults at different locations in the DC network. The faults F_3 and F_5 are simulated. PDs associated with the faults calculate the v_{RP} and compare to their respective thresholds. The dc circuit breaker operates and isolate the faulty section in both the cases, as shown in Fig. 9 and Fig. 10.

An autonomous mode of operation is simulated on RTDS to test the robustness and reliability of the proposed protection

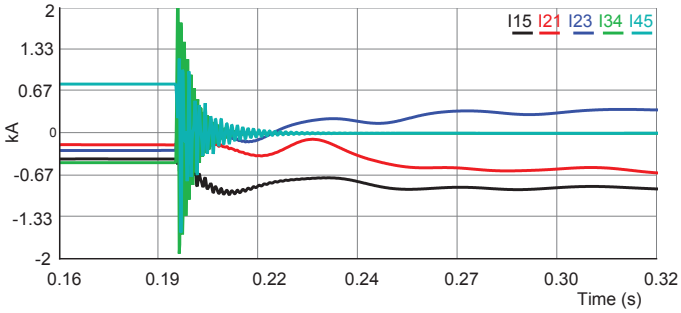

Fig. 9. Line currents after fault F_3 is cleared by $PD_{3.2}$ and $PD_{4.1}$

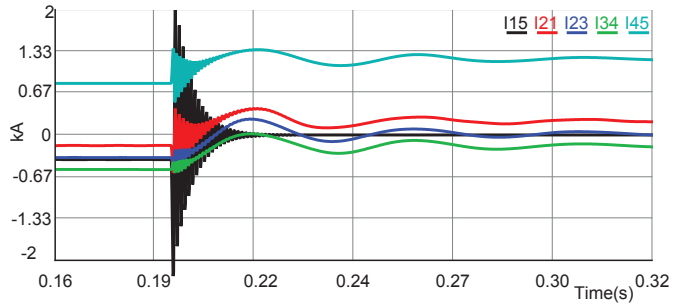

Fig. 10. Line currents after fault F_5 is cleared by $PD_{5.2}$ and $PD_{1.1}$

scheme. In this mode, the controller for the battery storage system was taken to be responsible for maintaining the DC grid voltage [14]. Since the total generation was less than the total connected load, the battery discharged to maintain the load bus voltage at 0.95 pu. Further, the fault F_2 was simulated and cleared by $PD_{2.2}$ and $PD_{3.1}$ as shown in Fig. 11. With this, only the selective part of the system gets disconnected. In this case, the current i_{21} and i_{23} become zero because of the unavailability of the AC source and presence of fault F_2. Due to the fast fault detection and isolation, the load bus voltage remains unaffected by the fault.

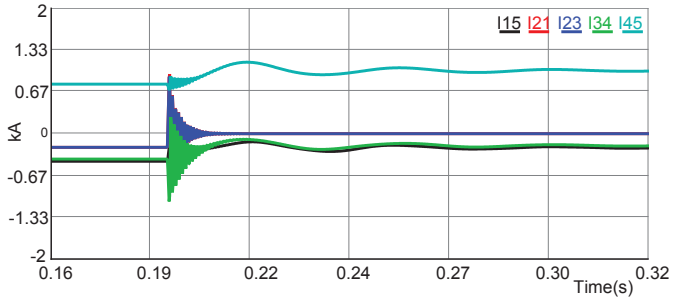

Fig. 11. Fault F_2 cleared by $PD_{2.2}$ and $PD_{3.1}$ in isanded mode

A. Performance with Noise in the Measurements

The proposed fault detection algorithm was further tested for the noise in the measurements. The voltage measurements were incorporated with the Gaussian noise having the standard deviation of 2.5% [15], [16], as shown in Fig. 12.

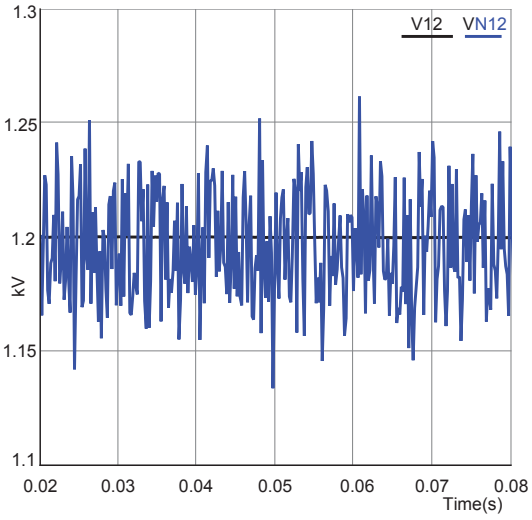

Fig. 12. Voltage measured by $PD_{1.2}$ incorporated with ($VN12$) and without noise ($V12$)

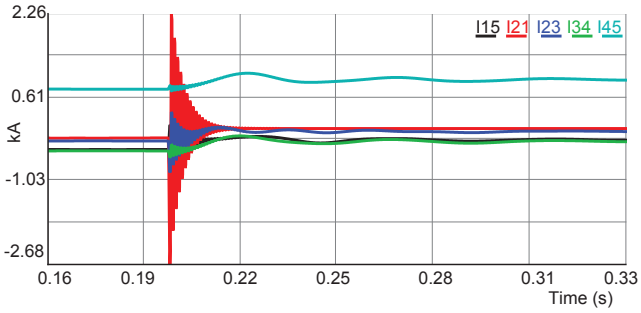

Fig. 13. Fault F_1 is cleared by $PD_{1.2}$ and $PD_{2.1}$ with noise in measurements

The fault F_1 was simulated in the noisy environment. The fault is accurately detected by $PD_{1.2}$ and $PD_{2.1}$ with the noise in the measured DC voltage, as shown in Fig. 13. It can be seen that the proposed algorithm is robust and is not affected by the noise simulated in the measurements.

B. Performance Comparison with Existing Schemes

Many schemes to detect fault in DC microgrids are available in literature [7], [8], [17]–[19], which detect and isolate the fault without de-energising the system. Few of the suggested schemes [17], [19] require a reliable communication to protect the system from fault. Generally, high bandwidth communication is required to detect the fault. Hence, these schemes are affected with communication network issues, such as packet loss, time delay etc.

In this section, the proposed protection scheme has been compared with an existing scheme which is based on local measurements [18]. This utilizes the overcurrent based protection scheme to detect the fault. The authors verified the

scheme for the multi-terminal DC radial architecture. The same scheme is implemented on the ring architecture of DC microgrid, as shown in Fig. 1.

The line to ground fault F_1 is simulated, which results into high fault current due to large filter capacitor and low cable impedance. It can be observed that the magnitude of both the current i_{21} and i_{23} are almost equal and may cause unwanted tripping of cable 2-3, as shown in Fig. 14a. This makes the relay coordination difficult. The level of difficulty increases as the inter connecting cable length reduces. Since, the current flow can be bidirectional in ring architecture, the relay coordination will becomes even more difficult.

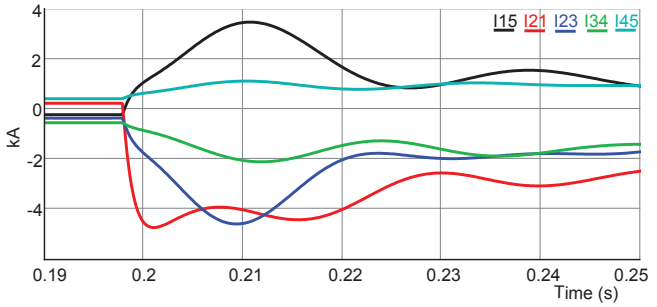

(a)

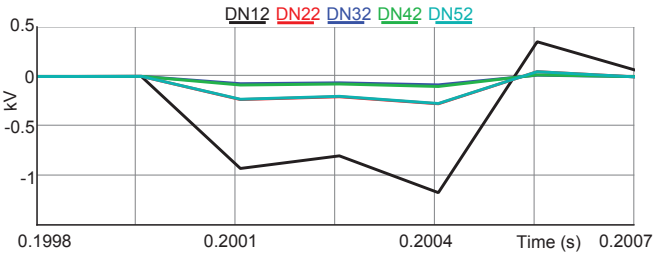

(b)

Fig. 14. (a) Current transients measured at $PD_{x.2}$ for fault F_1 (b) Voltages Δv_{RP} measured at $PD_{x.2}$ for fault F_1

The same fault F_1 is detected with the voltage prediction scheme. The change in predicted voltage is shown in Fig 14b. It can be seen that there is a significant difference in the voltage measured at $PD_{1.2}$ and at $PD_{2.2}$. In figure $DN12$, represents the difference in the predicted and the actual measured voltage Δv_{RP} at different PDs. This makes the fault detection and relay coordination easy. With the proposed scheme the fault is detected within 500μs and, hence, will reduce the breaker rating and its cost.

VII. Conclusion

The design of an effective protection system solution for a DC microgrid has been proposed in this paper. The characteristics of the voltage at the fault point is studied and a quadratic time dependent model is derived to mimic the voltage. The scheme is based on the local measurements and does not require any communication to detect the fault in system. The performance of the proposed scheme has been validated under various normal operating conditions, such as load variation and mode transition. Since the faults are associated with high dv/dt, the model takes few samples to track the voltage. The pick-up thresholds used in this work for fault detection are independent of the fault location and operating point of the microgrid. The validity of the proposed scheme has also been checked considering noise in the measured signal and found to remain unaffected of the noise. The proposed protection solution has been demonstrated for the loop type DC microgrid system. The scheme is easy to be extended to other configurations. The scheme is also verified and tested on the RTDS. The proposed scheme is fast in detecting and isolating the faulty section.

References

[1] R. H. Lasseter, "Microgrids," in *Proc. IEEE Power Engineering Society Winter Meeting*, vol. 1, no. 2, 2002, pp. 305–308.

[2] M. Starke, L. Tolbert, and B. Ozpineci, "Ac vs. dc distribution: A loss comparison," in *Proc. IEEE/PES Transmission Distribustion Conference Exposition*, 2008, pp. 1–7.

[3] D. Salomonsson, L. Soder, and A. Sannino, "Protection of low-voltage dc microgrids," *IEEE Trans. Power Del.*, vol. 24, no. 3, pp. 1045–1053, July 2009.

[4] M. Starke, L. Fangxing, L. M. Tolbert, and B. Ozpineci, "Ac vs. dc distribution: Maximum power transfer capability," in *Proc. IEEE/PES Conversion Delivery Electrctical Energy 21st Century*, 2008, pp. 1–6.

[5] L. Tang and B. Ooi, "Locating and isolating dc faults in multi-terminal dc systems," *IEEE Trans. Power Del.*, vol. 22, no. 3, pp. 1877–1884, July 2007.

[6] S. Fletcher, P. Norman, S. Galloway, and G. Burt, "Analysis of the effectiveness of non-unit protection methods within dc microgrids," in *Proc. IET Renewebale Power Generation, IET*, Sep 2011, pp. 1–6.

[7] S. D. A. Fletcher, P. J. N. andS. J. Galloway, P. Crolla, and G. M.Burt, "Optimizing the roles of unit and non-unit protection methods within dc microgrids," *IEEE Trans. Smart Grid*, vol. 3, no. 4, p. 20792087, Dec 2012.

[8] A. Meghwani, S. Srivastava, and S. Chakrabarti, "A new protection scheme for DC microgrid using line current derivative," in *Proc. IEEE/PES General Meeting*, 2015, pp. 1–5.

[9] K. Corzine, "Dc micro grid protection with the z-source breake," in *Proc. IEEE Industrial Electronics Conference, Vienna Austria*, Nov. 2013.

[10] A. H. Chang, B. R. Sennett, A.-T. Avestruz, S. Leeb, and J. L. Kirtley, "Analysis and design of dc system protection using z-source circuit breaker," *IEEE Trans. Power Electron.*, vol. 31, no. 2, pp. 1036 – 1049, 2016.

[11] A. Maeghwani, S. Srivastava, and S. Chakrabarti, "A non-unit protection scheme for DC microgrid based on local measurements," *IEEE Trans. Power Del.*, 2016.

[12] A. Meghwani, S. Srivastava, and S. Chakrabarti, "A new protection scheme for DC microgrid using line current derivative," in *Proc. IEEE/PES General Meeting*, 2015, pp. 1–5.

[13] A. Eisenberg and P.Pugliese, "Exact inversion of a class f vandermonde matrices," in *Proc. 5^{th} SIAM conference on applied algebra*, June 1994.

[14] P. H. Huang, P. C. Liu, W. Xiao, and M. S. E. Moursi, "A novel droop-based average voltage sharing control strategy for dc microgrids," *IEEE Trans. Smart Grid*, vol. 6, no. 3, pp. 1096–1106, 2015.

[15] R. Mohanty, U. S. M. Balaji, and A. K. Pradhan, "An accurate non-iterative fault-location technique for low-voltage DC microgrid," *IEEE Trans. Power Del.*, vol. 31, no. 2, pp. 475–481, 2016.

[16] J. G. Rao and A. K. Pradhan, "Power-swing detection using moving window averaging of current signals," *IEEE Trans. Power Del.*, vol. 30, no. 1, pp. 368–376, 2015.

[17] S. D. A. Fletcher, P. J. Norman, S. J. Galloway, P. Crolla, and G. M.Burt, "High speed differential protection for smart dc distribution system," *IEEE Trans. Smart Grid*, vol. 5, no. 5, pp. 2610–2617, 2014.

[18] M. E. Baran and N. R. Mahajan, "Overcurrent protection on VSC based multiterminal DC distribution systems," *IEEE Trans. Power Del.*, vol. 22, no. 1, pp. 406–412, 2007.

[19] J. D. Park, J. Candelaria, L. Ma, and K. Dunn, "DC ring-bus microgrid fault protection and identification of fault location," *IEEE Trans. Power Del.*, vol. 28, no. 4, pp. 2574–2584, 2013.